

Kinetics of Electron Attachment to Reverse Micelles

Young Jong Lee, Tieqiao Zhang, and Paul F. Barbara*

Department of Chemistry and Biochemistry, University of Texas at Austin, Austin, Texas 78712

Received: December 5, 2003; In Final Form: March 8, 2004

The kinetics of the attachment of isooctane solvated electrons to the water pools of reverse micelles (water/AOT/isooctane) has been studied by ultrafast time-resolved spectroscopy. The electrons generated in isooctane by photoionization (three photons of 400 nm) are observed to rapidly attach to reverse micelles, resulting in hydrated electrons in the water pools of the reverse micelles. The measured electron attachment rates (inferred from attachment yields) show a greater dependence on reverse micelle size than that predicted by a diffusion-controlled reaction model. Evidence is presented that highly delocalized, excess electron states of the water pool play an important role in the attachment process.

Introduction

Water and alkanes in the presence of surfactants exist in special cases as a homogeneous solution of a reverse micelle (RM) solute in the alkane solvent. Each RM is comprised of a water “core” surrounded by a surfactant layer. Alkane solvated electrons attachment to RM polar water pools have been extensively investigated as a route to the preparation of a hydrated electron in a confined water pool and a means for the investigation of electron donor/acceptor reaction kinetics across nonpolar/polar interfaces.^{1–6} For example, Bakale et al. measured the electron attachment rates to RMs in isooctane and tetramethylsilane solutions as a function of RM size using picosecond electron pulse conductivity.^{3,7} These measurements were made for the well-known water/AOT/alkane RM system, for which the RM size distribution is narrow^{8,9} and can be systematically varied by changing the molar ratio of water and surfactant, $W = [\text{H}_2\text{O}]/[\text{surfactant}]$.^{9–11}

The observed bimolecular electron attachment rates of Bakale et al. (approaching $10^{15} \text{ M}^{-1}\text{s}^{-1}$) are extraordinarily rapid compared to more typical bimolecular electron-transfer reactions in solution.^{3,7} Several factors appear to contribute to this rapid rate constant including, (i) an extraordinary large effective radius for alkane solvated electrons due to quantum delocalization, (ii) an extraordinary large diffusion constant for alkane solvated electrons compared to more typical electron donors, and (iii) an extraordinarily large radius of RMs compared to more typical electron acceptors. These various factors lead to large predicted diffusion controlled rate constants (the Smoluchowski equation) for alkane solvated electron attachment rates to RMs. The predicted rates are within an order of magnitude in many cases of the observed rates indicating that RMs are efficient alkane solvated electron acceptors. The observed rates do however exhibit significant discrepancies from the Smoluchowski equation, suggesting that the observed rates offer information on the size dependence of the electron acceptor properties of the RM.

The RM is a unique “electron acceptor” with many features different from typical molecular acceptors. For typical electron acceptors, electron attachment proceeds through a low-lying lowest unoccupied molecular orbital (LUMO) and additionally often involves the subsequent fragmentation to form a stable

anion, such as chloride. For the RM case, the solvated electron ultimately is attached to the water pool, which contains up to hundreds of thousands of water molecules and is surrounded by a close-packed surfactant layer. Individual water molecules are, in fact, poor electron acceptors with high-lying LUMO energies. In the water pool, however, the solvated electron ultimately is trapped in the form of a stable equilibrated s state hydrated electron in a water cavity. The attachment process to the RM may be analogous to the trapping and solvation of “conduction band” electrons in bulk water, which involves “excess electron states”, and proceeds by a cascade involving a delocalized conduction band at early times followed by relaxation to lower energy localized p and s states. Thus, the conduction band, p state, and s state may all participate in RM electron attachment depending on energetic and spatial factors.

In this work, ultrafast pump–probe spectroscopy on a water/AOT/ isooctane RM solution is used to generate isooctane-solvated electron/hole pairs ($e_{\text{iso}}^-/\text{hole}$) and to measure the subsequent dynamics, which involves a competition between $e_{\text{iso}}^-/\text{hole}$ geminate recombination and e_{iso}^- attachment to the RM. The observed dependence of the e_{iso}^- attachment yield on RM size is shown to vary cubically with RM radius suggesting that electron attachment proceeds through excess electron states of the water pool.

Experimental Section

The femtosecond laser system for the pump–probe transient absorption spectroscopy has been described earlier.^{12,13} Briefly, a multipass amplified Ti:sapphire system produced 35 fs pulses centered at 800 nm at a 1 kHz repetition rate. The laser beam was divided into two beams. The first beam was doubled (400 nm, 20 $\mu\text{J}/\text{pulse}$) and weakly focused on the sample with a diameter of 80 μm to ionize isooctane. The second beam generated a white light continuum, from which 650 nm was pre-selected, compressed by a prism pair, and used as a probe. The instrument response (fwhm) of 60 fs was used to fit the measured data.

AOT (Aerosol OT, sodium bis(2-ethylhexyl)sulfosuccinate, Aldrich) and isooctane (Aldrich) were purchased and used without any further purification. Water was deionized by a Barnstead system. The molar ratio, W , was varied from 7 to 50. All solutions form the RM phase (L_2) in the phase diagram of $\text{H}_2\text{O}/\text{AOT}/\text{isooctane}$.¹⁴ RM concentrations were calculated

* To whom correspondence should be addressed. E-mail: p.barbara@mail.utexas.edu.

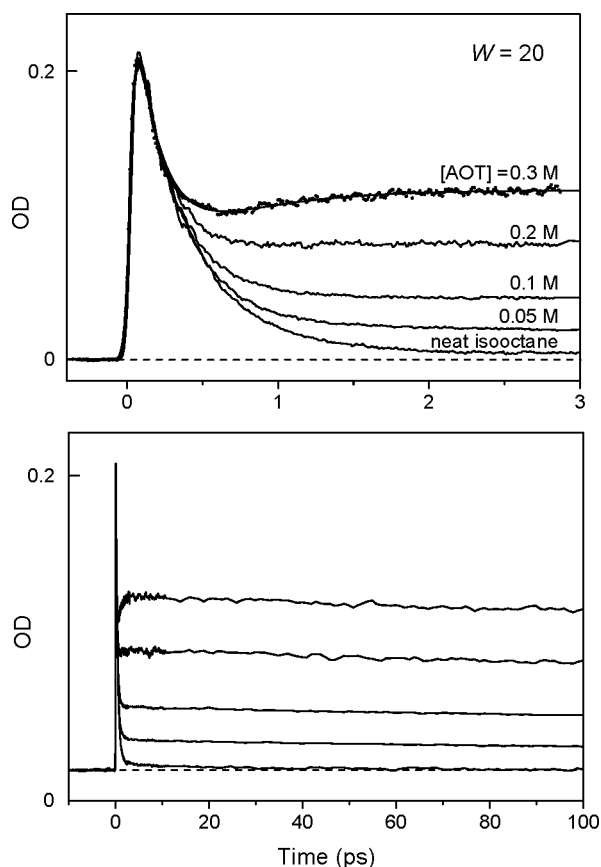


Figure 1. Comparison of the transient absorption of neat isooctane and RM solutions having different concentrations. The wavelengths of the ionization and probe pulses are 400 and 650 nm, respectively. The data of neat isooctane is well fitted with two exponentially decaying functions ($\tau_1 = 400$ fs, $A_1 = 0.97$; $\tau_2 = 39$ ps, $A_2 = 0.03$). The data of RM solutions are fitted with a triexponential function. For example, the data of $W = 20$ and $[AOT] = 0.3$ M is fitted with $\tau_1 = 160$ fs, $A_1 = 1.0$; $\tau_2 = 510$ fs, $A_2 = -0.3$; and $\tau_3 = 100$ ns, $A_3 = 0.33$.

by the usual procedure from $[AOT]$, W , and estimates of the radius of the RM water pool, $R_w(\text{\AA}) = 1.5 \times W$.^{9–11} All measurements were done with freshly made water/AOT/isooctane solutions to avoid buildup of any possible photoproducts and composition change by evaporation. Solutions were flowed using a gravity-driven wire-guided jet nozzle¹⁵ with a thickness of 80 ± 20 μm . The solution temperature was maintained at ambient temperature of 23 $^\circ\text{C}$.

Results and Discussion

Figure 1 shows transient optical density, $OD(t)$, data for various RM solutions with an intense pump pulse at 400 nm and a weak probe pulse at 650 nm. Immediately after the pump pulse in Figure 1, a prompt absorption is observed in all cases due to rapid formation (< 50 fs) of isooctane electron/hole pairs ($IP = 8.4$ eV)¹⁶ generated by the 400 nm pump pulse by 3-photon ionization (9.3 eV). The transient data for neat isooctane are relatively simple involving predominantly e_{iso}^- /hole geminate recombination on the ~ 400 fs time scale forming mostly ground-state isooctane and a small yield of isooctane excited states, as described elsewhere.^{17,18} In the presence of RMs the data are more complex due to a combination of kinetic processes including geminate recombination, e_{iso}^- attachment to the RM, and relaxation of hydrated electrons, e_{aq}^- , in the water pool (which occurs on the ~ 500 fs time scale and is a rising OD component).¹² The 650 nm probe pulse is capable of probing absorption bands of multiple species, i.e., the isooctane

hole, the isooctane excited state, e_{iso}^- in isooctane, and e_{aq}^- in the RM.

The long-lived ($\gg 100$ ps) absorption in the presence of RMs is assigned to e_{aq}^- in the RM water pool. The $\gg 100$ ps lifetime of this absorption component is consistent with reports of an e_{aq}^- /RM lifetime of hundreds of nanoseconds,^{2,4,6} from pulse radiolysis of RM solutions^{1–4} and, independently, by photoionization experiments on RMs that contain dissolved electron donors, e.g. phenothiazine.⁶ For large AOT concentrations (e.g., $[AOT] = 0.3$ M in Figure 1), the transient data occurs roughly on three time scales. At the earliest time scale, a decay is observed in the absorption signal because of disappearance of e_{iso}^- by a combination of competitive geminate recombination and attachment to RMs. At intermediate time, the OD actually increases slightly, as a result of e_{aq}^- relaxation in the RM water pool. At long times, the OD is a measure of the e_{aq}^- attachment yield and is constant as a function of time because of the long e_{aq}^- lifetime. The $OD(t)$ data measured at 650 nm were fit with an empirical triexponential function with relaxation times (τ_1 , τ_2 , and τ_3) and amplitudes (A_1 , A_2 , and A_3) with the third component representing the long-lived absorption due to e_{aq}^- . On the time scale of the electron attachment process to the RM, the relative cation/RM separations should be constant since the cation has an approximately 1000 times smaller mobility than the electron.¹⁹ Thus, the cations are not expected to influence the yield of electron attachment.

The complexity of the data makes it difficult to extract actual rate constants over the range of conditions. Instead, we have restricted the analysis to yields the fractional attachment yield (F_{RM}) of electrons by RMs, which is given by

$$F_{\text{RM}} = R_e(A_3/\Sigma A_i) \quad (1)$$

where R_e is the ratio of extinction coefficients for e_{iso}^- to e_{aq}^- at 650 nm, and $A_3/\Sigma A_i$ is the fractional amplitude of the long-lived kinetic component. By using the known extinction coefficients of the solvated electron in *n*-hexane²⁰ and bulk water,²¹ as approximate values for the required quantities, R_e is estimated to be ~ 0.3 , leading to a range of F_{RM} values shown in Figure 2. The yields, F_{RM} , in Figure 2 are within an order-of-magnitude of yields, F_{HR} , calculated using a homogeneous reaction model for the yield and the bimolecular scavenging rate constants (k_A) of Bakale et al.³

$$F_{\text{HR}} = \frac{k_A[\text{RM}]}{k_{\text{GR}} + k_A[\text{RM}]} \quad (2)$$

Since R_e is only an approximate value, we will emphasize below the functional dependence of F_{RM} on RM size and concentration rather than the actual magnitude the F_{RM} values.

Figure 2 shows that F_{RM} has a linear dependence on RM concentration at fixed RM size within experimental error. A linear dependence is consistent with previous experiments on electron scavenging from geminate electron/hole pairs, such as isooctane-solvated electrons scavenging by C_2HCl_3 ¹⁸ and hydrated electron scavenging by nitrate and other electron acceptors.¹³ (Interestingly, an approximately linear dependence of yield vs scavenger concentration is expected for yields $\ll 1$ whether the reaction is homogeneous or inhomogeneous with respect to the number of scavengers per electron/hole pair.)^{13,22} For isooctane, the diffusion length ($[D_e t]^{1/2}$) during the geminate recombination time of 400 fs is approximately 25 \AA based on the estimated diffusion constant ($D_e = 0.14 \text{ cm}^2\text{s}^{-1}$) from the Einstein relation ($D_e = \mu_e k_B T/e$) and the measured electron mobility ($\mu_e = 5.6 \text{ cm}^2\text{V}^{-1}\text{s}^{-1}$) in isooctane.²³ The mean RM

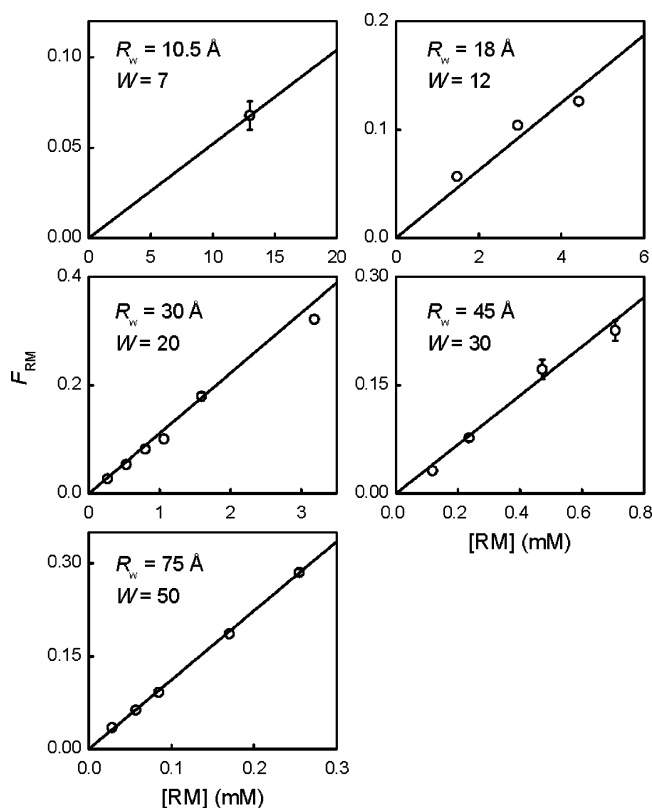


Figure 2. Measured F_{RM} at different $[RM]$ and W using eq 1 with R_e of 0.3. The measured F_{RM} show a good linearity with $[RM]$.

edge-to-edge separation for the typical concentration in this study is 50–150 Å demonstrating that the reaction is probably inhomogeneous with respect to the RM concentration.

One potential complication in measuring the attachment yields in these experiments is a competitive route for RM/hydrated electron formation due to direct photoionization of water in a RM^+ by three photons of 400 nm to produce an electron/hole pair in the water pool.^{24,25} To explore the contribution of e_{aq}^- from direct photoionization of water, OD values of neat water and RM solutions were successively measured with the same experimental configuration. With the volume fraction of water in the RM solution considered, a contribution from water photoionization is estimated to be 8% ($W = 12$) to 15% ($W = 50$). This relatively small effect has been ignored in the analysis and would not change the conclusions of this paper. Furthermore, the 8–15% estimate may be an over estimate since excitation of photoionization produced hydrated electrons by the trailing edge of the intense photoionization pulse²⁴ would tend to reduce the concentration of hydrated electrons due to excited-state reactions with the AOT.²⁶ Moreover, if this route were a major factor, a noticeable decay of RM hydrated electrons on the picosecond time scale is expected due to geminate recombination of hydrated electrons and water holes. This should be especially evident for the smaller RMs for which water pool electron/hole separations should be restricted to <10 Å. The absence of such a recombination signal for the data reported herein suggests that the direct route can probably be neglected for these experiments.

The slopes, S_{RM} , of the measured F_{RM} vs $[RM]$ in Figure 2 represent the acceptor propensity for a given RM size. Figure 3 portrays how S_{RM} (solid circles) depends on R_w in the form of a semi-log plot. The S_{RM} data shows a surprisingly large dependence on R_w that is well-fit by a cubic curve (solid-line). Interestingly, the previously measured bimolecular rate constants

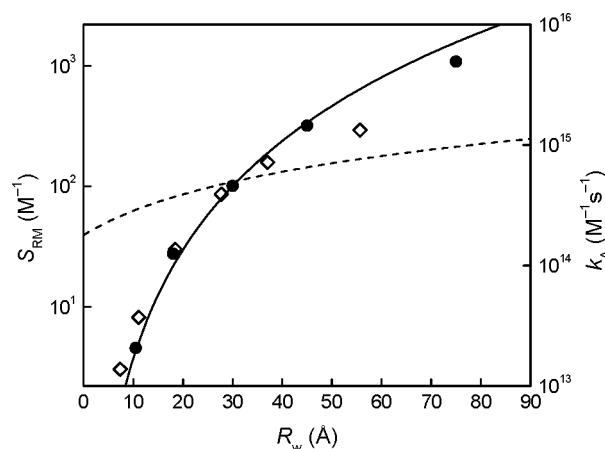


Figure 3. Comparison of the measured and calculated reaction rate constants. The dotted line is calculated from the simple diffusion-limited reaction model (eq 3), where $R_e = 17$ Å.^{3,28} The slopes S_{RM} (solid circles) determined from the measured F_{RM} show a greatly similar R_w dependence to the measured bimolecular reaction rate constants of Bakale et al.³ (diamonds), which are recalculated using $R_w(\text{Å}) = 1.5 \times W$. The solid line is $A \times R_w^3$, using a best-fit value, $A = 3.7 \times 10^{-3} \text{ M}^{-1} \text{ Å}^{-3}$. The Schulz size distribution with the polydispersity ($\sigma/R_{ave} = 0.2$)³¹ is convoluted for all RM solutions before fitting.

(diamonds) for electron scavenging by RMs of Bakale et al.^{3,7} closely parallel the scavenging yield data supporting the kinetic origin of the R_w trends in the yield data. We use the radius of the water pool (R_w) rather than the radius of the RM (R_w + the length of carbon chains),^{3,7} because the RM carbon chains (isooctyl) of the AOT surfactant are similar to the solvent (isooctane) and should not affect the scavenging reaction.

A cubic dependence on R_w is much greater than that predicted for a diffusion-controlled electron attachment (dashed-line in Figure 3). This line was calculated assuming that the yield is linearly proportional to rate. The rate was calculated, as follows:

$$k_A(R_w) = 4\pi(D_e + D_{RM})(R_w + R_e) \quad (3)$$

where D_{RM} is the diffusion coefficient of a RM. ($D_e + D_{RM}$) can be replaced with D_e , since D_{RM} is several orders of magnitude smaller than D_e .²⁷ The radius of e_{iso}^- , R_e , was taken to be 17 Å, which is the estimated upper limit in isooctane at 293 K.^{3,28}

A potential factor that may explain the unexpected cubic dependence of the solvated electron scavenging ability of a RM water pool on R_w is the “excess electron” density of states of the water pool. Based on the results of calculations on excess electrons in water clusters and, independently, bulk water, it is reasonable to conclude that the number of energetically accessible excess electronic states of a water pool increases approximately cubically with R_w . In other words, an excess electron in the alkane phase interacts with highly delocalized, excess electron states of the water pool during the attachment process to a RM. In turn, this should accelerate the attachment process through a greater virtual electron density on the RM during the attachment step. The excess electron states can be roughly divided into low energy localized (s and p) states due to preexisting cavities²⁹ in the water pool and higher-energy delocalized conduction band states.³⁰ Theoretical guidance and further experiments will be necessary to determine which type of excess electron state plays a bigger role in electron scavenging. Thus, the cubic dependence reported herein is strong evidence that the water pool excess electron states are critical to the attachment process.

Conclusion

The kinetics of the attachment of isooctane solvated electrons to the water pools of reverse micelles (water/AOT/isooctane) has been studied by ultrafast time-resolved spectroscopy. The electrons generated in isooctane by photoionization (three photons of 400 nm) are observed to rapidly attach to reverse micelles, resulting in hydrated electrons in the water pools of the reverse micelles. The measured electron attachment rates (inferred from attachment yields) show a greater dependence on RM size than that predicted by a diffusion-controlled reaction model, perhaps as a result of intermediacy of excess electron states of the water pool in the attachment process.

Acknowledgment. We acknowledge support of this research by the Basic Energy Sciences Program of the Department of Energy and the Robert A. Welch Foundation.

References and Notes

- (1) Wong, M.; Graetzel, M.; Thomas, J. K. *Chem. Phys. Lett.* **1975**, *30*, 329.
- (2) Pileni, M. P.; Hickel, B.; Ferradini, C.; Pucheault, J. *Chem. Phys. Lett.* **1982**, *92*, 308.
- (3) Bakale, G.; Beck, G.; Thomas, J. K. *J. Phys. Chem.* **1992**, *96*, 2328.
- (4) Gebicki, J. L.; Gebicka, L.; Kroh, J. J. *Chem. Soc., Faraday Trans.* **1994**, *90*, 3411.
- (5) Gauduel, Y.; Pommeret, S.; Yamada, N.; Migus, A.; Antonetti, A. *J. Am. Chem. Soc.* **1989**, *111*, 4974.
- (6) Calvo-Perez, V.; Beddard, G. S.; Fendler, J. H. *J. Phys. Chem.* **1981**, *85*, 2316.
- (7) Bakale, G.; Beck, G.; Thomas, J. K. *J. Phys. Chem.* **1981**, *85*, 1062.
- (8) Arleth, L.; Pedersen, J. S. *Phys. Rev. E* **2001**, *6306*, 061406.
- (9) Kotlarchyk, M.; Stephens, R. B.; Huang, J. S. *J. Phys. Chem.* **1988**, *92*, 1533.
- (10) Pileni, M. P.; Zemb, T.; Petit, C. *Chem. Phys. Lett.* **1985**, *118*, 414.
- (11) Hirai, M.; Kawai-Hirai, R.; Takizawa, T.; Yabuki, S.; Nakamura, K.; Hirai, T.; Kobayashi, K.; Amemiya, Y.; Oya, M. *J. Phys. Chem.* **1995**, *99*, 6652.
- (12) Son, D. H.; Kambhampati, P.; Kee, T. W.; Barbara, P. F. *Chem. Phys. Lett.* **2001**, *342*, 571.
- (13) Kee, T. W.; Son, D. H.; Kambhampati, P.; Barbara, P. F. *J. Phys. Chem. A* **2001**, *105*, 8434.
- (14) Tamamushi, B.; Watanabe, N. *Colloid Polym. Sci.* **1980**, *258*, 174.
- (15) Tauber, M. J.; Mathies, R. A.; Chen, X. Y.; Bradforth, S. E. *Rev. Sci. Instrum.* **2003**, *74*, 4958.
- (16) Casanovas, J.; Grob, R.; Delacroix, D.; Guelfucci, J. P.; Blanc, D. *J. Chem. Phys.* **1981**, *75*, 4661.
- (17) Sander, M. U.; Brummund, U.; Luther, K.; Troe, J. *J. Phys. Chem.* **1993**, *97*, 8378.
- (18) Zhang, T.; Lee, Y. J.; Kee, T. W.; Barbara, P. F. To be submitted for publication.
- (19) de Haas, M. P.; Warman, J. M.; Hummel, A. *Conduction and Breakdown in Dielectric Liquids*; The 5th International Conference on Conduction and Breakdown of Dielectric Liquids; Delft University of Technology: Delft, The Netherlands, 1975.
- (20) Baxendale, J. H.; Bell, C.; Wardman, P. *J. Chem. Soc., Faraday Trans. 1* **1973**, *69*, 776.
- (21) Hart, E. J.; Anbar, M. *The Hydrated Electron*; Wiley-Interscience: New York, 1970.
- (22) Pimblott, S. M.; LaVerne, J. A. *J. Phys. Chem. A* **1998**, *102*, 2967.
- (23) Holroyd, R. A. The Electron: Its Properties and Reactions. In *Radiation Chemistry. Principles and Applications*; Farhataziz; Rodgers, M. A. J., Eds.; VCH Publishers: New York, 1987.
- (24) Son, D. H.; Kambhampati, P.; Kee, T. W.; Barbara, P. F. *J. Phys. Chem. A* **2001**, *105*, 8269.
- (25) Crowell, R. A.; Bartels, D. M. *J. Phys. Chem.* **1996**, *100*, 17940.
- (26) Lee, Y. J.; Kee, T. W.; Zhang, T.; Barbara, P. F. *J. Phys. Chem. B* **2004**, *108*, 3474.
- (27) Zulauf, M.; Eicke, H. F. *J. Phys. Chem.* **1979**, *83*, 480.
- (28) Itoh, K.; Munoz, R. C.; Holroyd, R. A. *J. Chem. Phys.* **1989**, *90*, 1128.
- (29) Motakabbir, K. A.; Schnitker, J.; Rossky, P. J. *J. Chem. Phys.* **1992**, *97*, 2055.
- (30) Kee, T. W.; Lee, Y. J.; Barbara, P. F. To be submitted for publication.
- (31) Svergun, D. I.; Konarev, P. V.; Volkov, V. V.; Koch, M. H. J.; Sager, W. F. C.; Smeets, J.; Blokhuis, E. M. *J. Chem. Phys.* **2000**, *113*, 1651.